An Efficient Lattice Boltzmann Model for 3D Transient Flows

Raoudha Chaabane, Abdelmajid Jemni, and Fethi Aloui

Abstract In this paper, we report on the development and the implementation of the mesoscopic approach based on the Lattice Boltzmann method (LBM) in order to simulate three-dimensional coupled modes of thermal and fluid flows. First the lattice Boltzmann method (LBM) has been used to solve transient heat conduction problems in 3D Cartesian geometries. To study the suitability of the LBM, the problem has also been extended to deal with a coupled conduction-radiation heat transfer problem in a three-dimensional cavity containing an absorbing, emitting, and scattering medium. In this case, the radiative information is obtained by solving the radiative transfer equation (RTE) using the control volume finite element method (CVFEM). Second, a 3D incompressible thermal lattice Boltzmann model is proposed to solve 3D incompressible thermal flow problems. A D3Q19 particle velocity model is incorporated in our thermal model where the density, velocity, and temperature fields are calculated using the two double population lattice Boltzmann equation (LBE). It is indicated that the present thermal model is simple and easy for implementation. It is validated by its application to simulate the 3D natural convection of fluid in a cubical enclosure, which is heated differentially at two vertical side walls. In order to test the efficiency of the developed method, comparisons are made for the effect of Rayleigh number on the temperature and velocity distributions in the medium. Validation and the analysis of numerical results of flow and thermal fields in the cubic cavity are at Rayleigh numbers of 10^3–10^6. In all studied cases, it is found that the numerical results agree well with the results reported in previous studies. The 3D LBGK algorithm presented here can also be extended for a convective radiative problem in a three-dimensional grey participating medium in the presence of computers with sufficient memory and computational power to perform well-resolved calculations of the hybrid 3D-proposed model.

R. Chaabane · A. Jemni
National Engineering School of Monastir (ENIM), LESTE Laboratory, University of Monastir, Avenue Ibn El Jazzar, 5019 Monastir, Tunisia

F. Aloui (✉)
Université Polytechnique Hauts-de-France (UPHF), LAMIH, CNRS UMR 8201, INSA Hauts-de-France, 59313 Valenciennes, France
e-mail: fethi.aloui@uphf.fr

Keywords LBM · Conduction · Convection · Radiation

1 Introduction

Numerical modelling of the coupled steady conduction or convection and radiation heat transfer problem has been an area of great interest because of its broad applications in engineering. It has numerous applications in the area of fire protection, glass processing, industrial furnaces, Fuel cell, and optical textile fibre processing [1].

Nowadays, solutions of multidimensional transient conductive and radiative transfer are an active research subject because of their practical and interesting engineering applications. Several works are available dealing with combined conduction and radiation heat transfer in 1D and 2D geometries [2–6]. Interaction of transient conduction radiation was found to be interesting, and ignoring one of these modes could result considerable deviation from real situation. The LBM-CVFEM [6] shows very successful results from the viewpoint of accuracy, grid, and CPU time compatibility. It is proved to be a reliable future numerical tool for combined heat transfer problems in engineering applications.

2 Numerical Analysis

Lattice Boltzmann method appears as a powerful mesoscopic tool for solving Energy problems in complex geometries. Modelling different transport phenomena that occur inside energetic systems have been gaining interest during the last years. The most realistic model has to be a 3-dimensional, non-steady state and with the coupling of the different transport phenomena over all the range of scales from the micro- to the macroscale. When modelling energetic systems at micro or macro scale, it is important to deeply understand the behaviour of the fluids throughout the media present in the different layers of the energetic configuration geometry. Then solving transport phenomena in more realistic complex geometries is considered one of the problems to deal with. Lattice Boltzmann method (LBM) can handle with problems at different scales and has proven to be suitable for solving problems in wide range of energetic configurations media, and modelling different transport phenomena in such complex area of energy research. The aim of this work is to show the solution of physical problems using the LBM.

3 Conduction Radiation

The unsteady energy conservation equation consisting of conduction and radiation can be expressed as

$$\rho c_p \frac{\mathrm{d}T}{\mathrm{d}t} = \nabla.(k\nabla T - \overrightarrow{q_R}) \tag{1}$$

It is assumed that the thermal conductivity k of the emitting, absorbing, and scattering medium is independent of temperature. ρ is the density, c_p is the specific heat, and $\overrightarrow{q_R}$ represents the radiative heat flux given by:

$$\overrightarrow{q}_R = \int_{4\pi} I\overrightarrow{\Omega}d\Omega \tag{2}$$

where I is the radiative intensity which can be obtained by solving the Radiative Transfer Equations (RTE).

The divergence of radiative heat flux is given by

$$\overrightarrow{\nabla}.\overrightarrow{q}_R = k_a(4\pi I_b - G) \tag{3}$$

$I_b = \sigma T^4/\pi$ is the blackbody intensity, G is the incident radiation and k_a is the absorption coefficient.

For the RTE, an absorbing, emitting, and scattering grey medium can be written as

$$\overrightarrow{\nabla}.(I(s, \overrightarrow{\Omega}).\overrightarrow{\Omega}) = -(k_a + k_d)I(s, \overrightarrow{\Omega}) + k_a I_b(s)$$
$$+ (k_d/4\pi) \int_{\Omega'=4\pi} I(s, \overrightarrow{\Omega'})\Phi(\overrightarrow{\Omega'} \rightarrow \overrightarrow{\Omega})d\Omega' \tag{4}$$

where $I(s, \overrightarrow{\Omega})$ is the radiative intensity, which is a function of position s and direction $\overrightarrow{\Omega}$; k_d is the scattering coefficient, and $\Phi(\overrightarrow{\Omega'} - \overrightarrow{\Omega})$ is the scattering phase function from the incoming $\overrightarrow{\Omega'}$ direction to the outgoing direction $\overrightarrow{\Omega}$.

The term on the left-hand side represents the gradient of the intensity in the direction. The three terms on the right-hand side represent the changes in intensity due to absorption and out-scattering, emission, and in-scattering, respectively [6–9]. The radiative boundary condition for Eq. (4), when the wall bounding the physical domain is assumed grey and emits and reflects diffusely, can be expressed as

$$I_w(\overrightarrow{\Omega}) = (\varepsilon_w \sigma T_w^4/\pi)$$
$$+ ((1 - \varepsilon_w)/\pi) \int_{\overrightarrow{\Omega'}.\overrightarrow{n}_w<0} I_w(\overrightarrow{\Omega'})\left|\overrightarrow{\Omega'}.\overrightarrow{n}_w\right|d\Omega' \text{ if } \overrightarrow{\Omega'}.\overrightarrow{n}_w > 0 \tag{5}$$

$\overrightarrow{n}_w$ is the unit normal vector on the wall, and ε_w represents the wall emissivity [10, 11].

In the LBM, the equation describing transient conduction-radiation heat transfer [12–19] is:

$$f_i(\vec{r} + \vec{c_i}\,\Delta t, t + \Delta t) = f_i(\vec{r}, t) - \frac{\Delta t}{\tau}[f_i(\vec{r}, t) - f_i^{(0)}(\vec{r}, t)]$$

$$- (\frac{\Delta t}{\rho c_p})w_i(\nabla.\vec{q_R}(\vec{r}, t)) \quad i = 0, .., 18 \qquad (6)$$

$$\tau = \frac{3\alpha}{|\vec{e_i}|^2} + \frac{\Delta t}{2} \qquad (7)$$

The velocities $\vec{e_i}$ and their corresponding weights ω_i in the D3Q19 (Fig. 1) lattice are the following:

$$\vec{e}_0 = (0, 0, 0),\ \vec{e}_{1,2} = (\pm1, 0, 0).C,\ \vec{e}_{3,4} = (0, \pm1, 0).C,$$
$$\vec{e}_{5,6} = (0, 0, \pm1).C,\ \vec{e}_{7...10} = (\pm1, \pm1, 0).C,$$
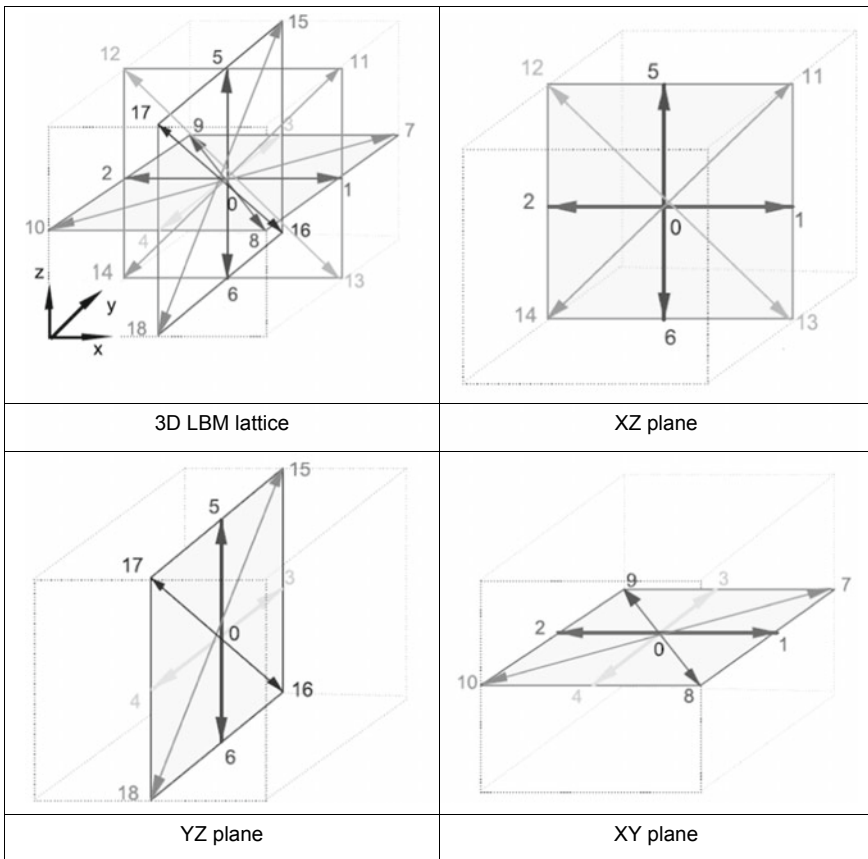
Fig. 1 D3Q19 LBM projection discretisation scheme

$$\vec{e}_{11...14} = (\pm 1, 0, \pm 1).C, \; \vec{e}_{15...18} = (0, \pm 1, \pm 1).C \tag{8}$$

$$\omega_0 = \frac{1}{6}, \; \omega_{1...6} = \frac{1}{18}, \; \omega_{7....18} = \frac{1}{36} \tag{9}$$

In the present problem, temperature is computed from

$$T(\vec{r}, t) = \sum_{i=0}^{b} f_i(\vec{r}, t) \tag{10}$$

To process Eq. (6), the required equilibrium distribution $f_i^{(0)}$ is given by

$$f_i^{(0)}(\vec{r}, t) = \omega_i T(\vec{r}, t) \tag{11}$$

The energy equation is subjected to Dirichlet boundary condition. To express this condition, the bounce-back concept in the LBM in which particle fluxes are balanced at any point on the boundary was used. For 1D and 2D geometries, implementations of the temperature boundary conditions in the LBM have been explained in the literature [12]. In the present work, procedures described in [12] have been followed.

4 Free Convection

The geometry and the coordinate system are illustrated in Fig. 2. The enclosure is simply represented by a rectangular prism with the height H, width, and length L.

Fig. 2 The geometry and the coordinate system of cubic enclosure
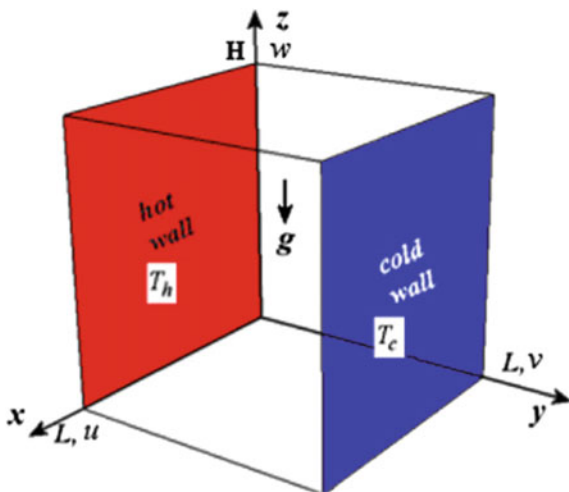
The left and right lateral walls, as shown in Fig. 12, are kept at uniform T_h and T_c, respectively. Other walls are assumed to be adiabatic. The temperature difference between the hot and cold surfaces promotes the buoyancy driven flow inside the enclosure. The temperature difference is also assumed to be small enough so that the Boussinesq approximation is valid.

The known CFD steady state equations for a Newtonian fluid for continuity, the momentum equations, and the energy equation will be simulated by the mesoscopic approach (LBM).

For computation of density and velocity fields, the governing lattice Boltzmann equation is given by [1, 16, 17].

$$
\begin{aligned}
f_k(\overrightarrow{r} + \overrightarrow{c_k}\Delta t, t + \Delta t) &= f_k(\overrightarrow{r}, t) \\
&- \frac{\Delta t}{\tau_v}[f_k(\overrightarrow{r}, t) - f_k^{\mathrm{eq}}(\overrightarrow{r}, t)] + \Delta t\, F, \quad k = 0, .., 8
\end{aligned}
\tag{12}
$$

where f_k are the particle distribution function defined for the finite set of the discrete particle velocity vectors $\overrightarrow{c_k}$. The collision term Ω_k on the right-hand side of Eq. (12) uses the so-called BGK approximation [18].

Where f_k^{eq} is the local equilibrium distribution function that has an appropriately prescribed functional dependence on the local hydrodynamic properties and τ_v is the relaxation time defined as:

$$
\tau_v = \frac{1}{2} + \frac{3\nu}{c^2 \Delta t}
\tag{13}
$$

F represents the external force term given by:

$$
F = \left[\frac{(\rho \beta_T g (T - T_m)\overrightarrow{j}).(\overrightarrow{c_k} - \overrightarrow{u})}{RT} \right] f_k^{\mathrm{eq}}
\tag{14}
$$

where the unit vector $\overrightarrow{j}$ is in a direction opposite to gravity, T_m is the mean temperature, g is the gravity acceleration, β_T is the volumetric thermal expansion coefficient and ρ is the density of the fluid at the mean temperature.

The macroscopic density ρ and the velocity $\overrightarrow{u}$ are calculated as follow:

$$
\rho(\overrightarrow{r}, t) = \sum_k f_k(\overrightarrow{r}, t)
\tag{15}
$$

$$
\overrightarrow{u}(\overrightarrow{r}, t) = \sum_k \overrightarrow{c}_k f_k(\overrightarrow{r}, t)/\rho(\overrightarrow{r}, t)
\tag{16}
$$

5 Results and Discussions

5.1 Validation with Pure 3D Transient Conductive Case

In a pure transient heat conduction transfer problems, a 3D cubical enclosure of unit length is considered. With a D3Q19 lattice Boltzmann method, steady state conditions were assumed to have been achieved when the temperature difference between two consecutive time levels at each lattice centre did not exceed 10^{-6}. Non-dimensional time was defined as $(\xi = \alpha\beta^2 t)$, and $\Delta\xi$ was taken as 10^{-4}. To check the accuracy of the present D3Q19 LBM algorithm, results are compared with results of literature using a D3Q15 LBM algorithm [19]. In this case, initially the initial condition is $T(x, y, z, 0) = T_0$.

The imposed boundaries conditions are $T(x, y, Z, t) = T(0, y, z, t) = T(0, y, z, t) = T(0, y, z, t) = T(X, y, z, t) = T(x, 0, z, t) = T(x, Y, z, t) = T_0$ and $T(x, y, 0, t) = T_{hot}$.

In the present D3Q19 LBM algorithm, boundary temperatures $T_{hot} = T_{ref}$ and other walls are at $T_i = 0.25 T_{ref}$. In Fig. 3, results are generated for $31 \times 31 \times 31$ lattices.

In Fig. 3, the T/T_{ref} results of the steady state D3Q19 LBM algorithm and the reference's ones have been compared along the centreline $(y/Y = 1/2)$ in the $y - z$ plane at $(x/X = 1/2)$. A good agreement is found as seen from the transient non-dimensional temperature plots at different instants $\xi = 0.001$, $\xi = 0.01$, $\xi = 0.05$, and $\xi = \infty$. A given semi-transparent medium (SMT) can have a volumetric heat generation source, so effects of heat generation are compared and shown in Fig. 4.

Fig. 3 Centreline temperature along (z/Z) direction, validation with [19]
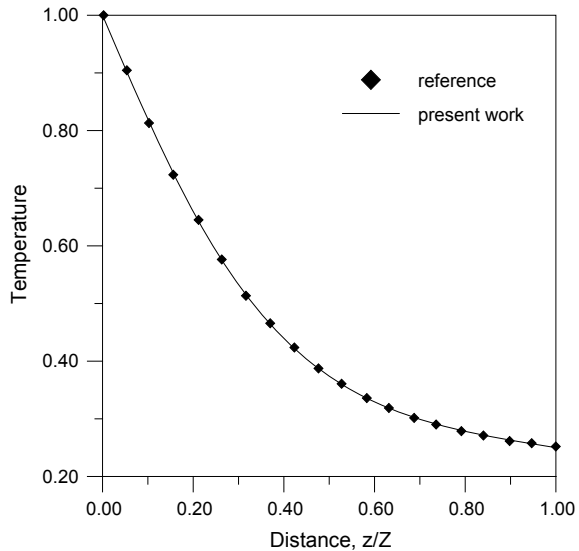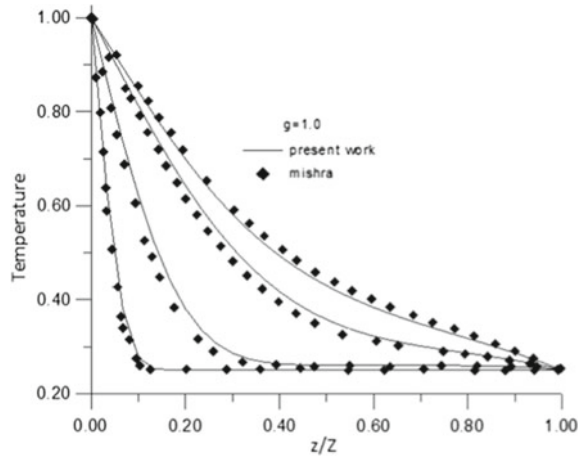
Fig. 4 Effect of heat
generation on centreline
non-dimensional
temperature distribution in a
3D enclosure

Results are plotted for the case of unity value of the non-dimensional heat generation
for different time ξ levels including the transient and the steady state. Results were
compared with literature [19]. It can be seen that the proposed algorithm presents an
accurate result.

5.2 Validation with Pure 3D Radiative Case

In order to assess the CVFEM algorithm with basic reliable cases, the numerical
approach was implemented for a cubical enclosure in which the medium is absorbing-
emitting with an emissive power of unity. All the walls are black and cold (0 K).
Solutions were obtained with ($11 \times 11 \times 11$) control volumes and (8×6) control
angles. Figure 5 shows the non-dimensional surface radiative flux along the centreline
of a wall. It compare the predicted flux distribution with that of the exact solution in
literature [11] and their benchmark code for $ke = 1$ m^{-1} and $ke = 10$ m^{-1}. It can
be seen that the proposed algorithm presents good results.

The second test case is made of a black-walled square box–shaped furnace
enclosure (1 m × 1 m × 1 m). The walls are cold and the medium is grey with
$\beta = 1$ m^{-1},$\omega = 0.5$. The results were obtained with ($11 \times 11 \times 11$) control volumes
and (8×6) control angles. The wall heat flux for absorbing-emitting and isotropically
scattering medium in the cubic enclosure is shown in Fig. 4b. The obtained results
are in good agreement with the reference result [19].

After validation with pure 3D conductive case (Figs. 3 and 4) and radiative
case (Figs. 5 and 6), the 3D transient conduction-radiation heat transfer problems
considered in the present work is highlighted based on the variation of the transient
and the steady temperature for various extinction coefficients (Fig. 7), conduction-
radiation parameters (Fig. 8), and scattering albedos (Fig. 9). One hot boundary is

Fig. 5 Wall heat flux for absorbing-emitting in the cubic enclosure $\beta = 0.1,\ \beta = 1,\ \beta = 10$ [11]
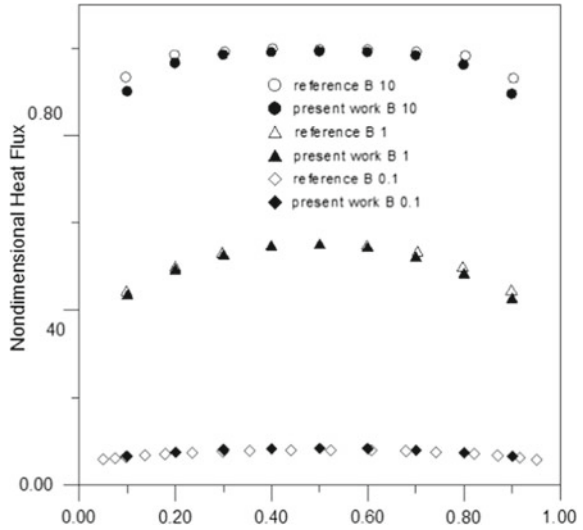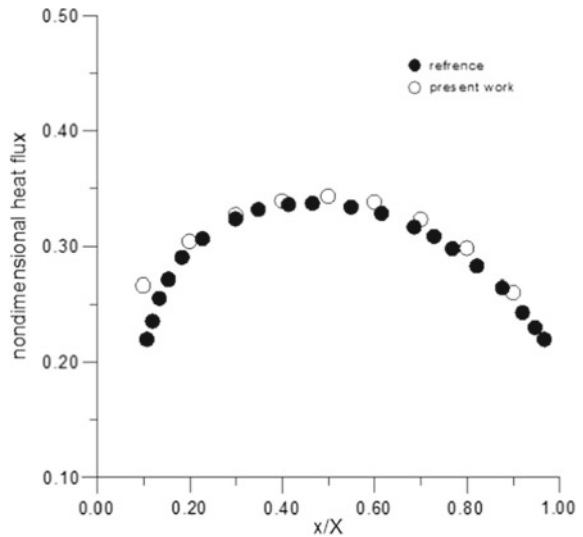

Fig. 6 Wall heat flux for absorbing-emitting and isotropically scattering medium in the cubic enclosure $\beta = 0.1,\ \beta = 1,\ \beta = 10$ [11]

at $\theta = T/T_{\text{hot}} = 1$, and others are at the same lower temperature $\theta = 1/2$. Results of temperature distributions along z/Z direction at $x/X = 1/2$ and $y/Y = 1/2$ are presented in Figs. 7, 8, and 9. A $15 \times 15 \times 15$ grid points and 8×6 rays are considered for all the cases. Results are presented in graphical form rather than tabular form so as to explain the physical trend more effectively.

In those figures, at different time levels, centreline ($x/X = 1/2$ and $y/Y = 1/2$) temperature distributions along the z/Z direction obtained from LBM-CVFEM have been highlighted for the effects of different radiative parameters.
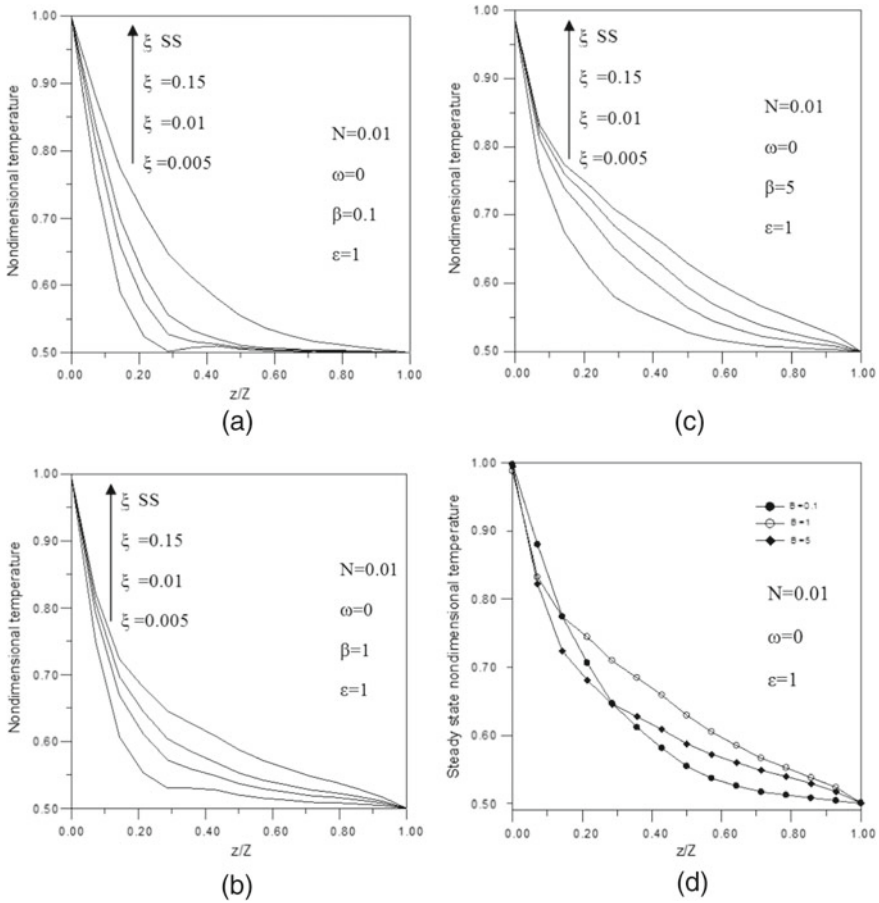
Fig. 7 Transient (**a–c**) and steady state (**d**) centreline ($x/X = y/Y = 1/2$) temperature: effect of the extinction coefficient

For black boundaries and for no scattering ($\omega = 0$), the effect of the extinction coefficient β is shown in Fig. 7 for $N = 0.01$. The temperature profile (Fig. 7a) for lower $\beta = 0.1$ approaches the pure conduction profile.

The influence of the conduction to radiation parameter $N = k\beta/4\sigma T_{hot}^3$ that characterizes the relative importance of conduction in regard to radiation is presented for temperature response in Fig. 8 for black boundaries and for no scattering.

It is shown (Fig. 8c) that the temperature profile is near to a pure conduction profile for $N = 1$ because it display a conduction-dominated situation showing higher temperature gradient. For $N = 0.01$(Fig. 8a), a comparatively flat profile is seen as medium temperature increases with lower temperature gradient.
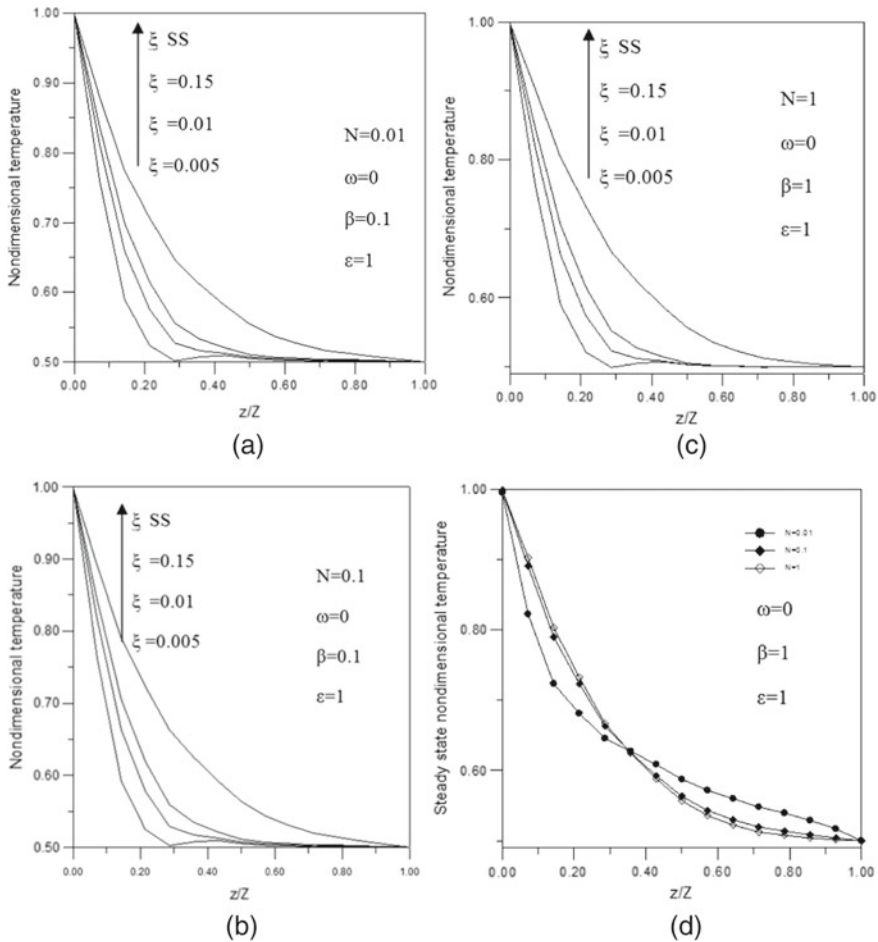
Fig. 8 Transient (**a–c**) and steady state (**d**) centreline ($x/X = y/Y = 1/2$) temperature: effect of the conduction-radiation parameter coefficient

For $N = 0.01$, $\beta = 1$, and perfectly black boundaries, the parametric study for the effect of the scattering albedo ω is highlighted in Fig. 9. The medium temperature comparatively increases for an absorbing-emitting medium ($\omega = 0$).

The computer code for the present 3D problem has been extended for transient convection and validated against the results given in literature [20] (Fig. 10); unsteady convection problem in a 3D real cubical enclosure has been considered. The continuity, momentum, and the energy equations are solved using the Lattice Boltzmann mesoscopic approach.

In Fig. 11, with Ra $= 10^3$ – Ra $= 10^6$ along z/Z and x/X direction at $y/Y = 0.5$ the centreline non-dimensional temperature has been highlighted. For a cubical medium undergoing transient convection, grid independence results are studied and Figs. 8,
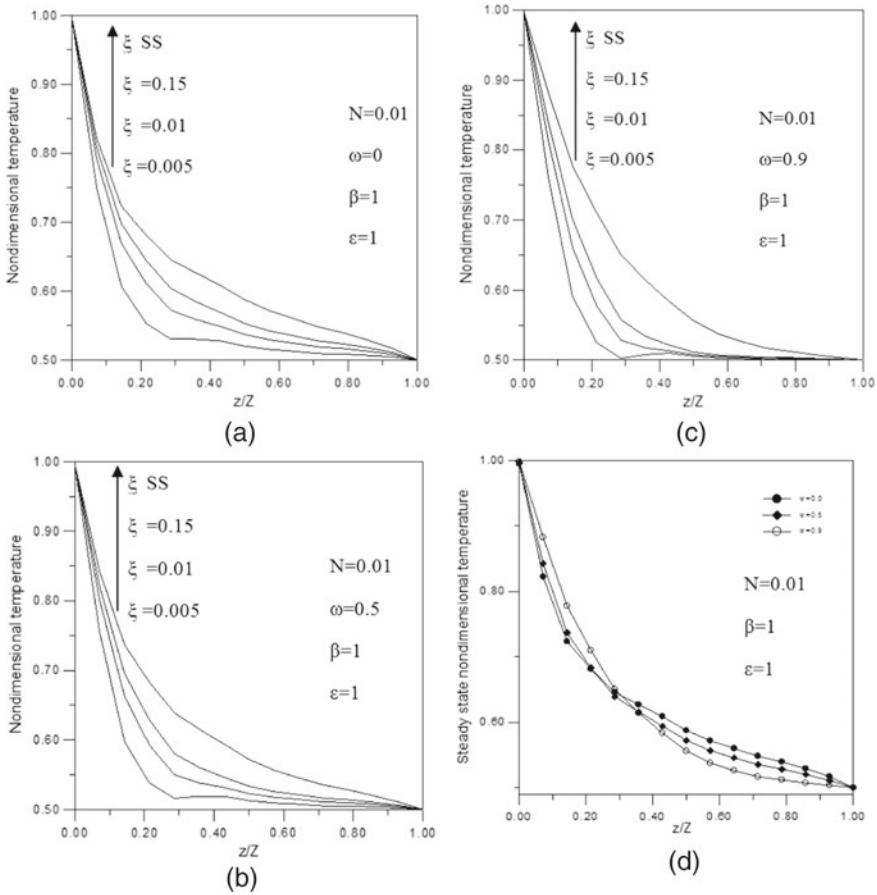
Fig. 9 Transient (**a–c**) and steady state (**d**) centreline ($x/X = y/Y = 1/2$) temperature: effect of the scattering albedo coefficient

9, and 10, respectively, show centreline temperature along z/Z direction at $x/X = 0.5$ and $y/Y = 0.5$ of the cubical medium for 155 * 155 * 155 lattices and iso-surfaces of temperature for $Ra = 10^6$ (Figs. 12 and 13).

6 Conclusions

LBM-CVFEM was used for the solution of unsteady combined conduction-radiation problems in a 3D cubical absorbing, emitting, and isotropically enclosure. Centreline temperature distributions were obtained for various parameters. The convective results presented in this study highlight the efficiency and the robustness of LBM and
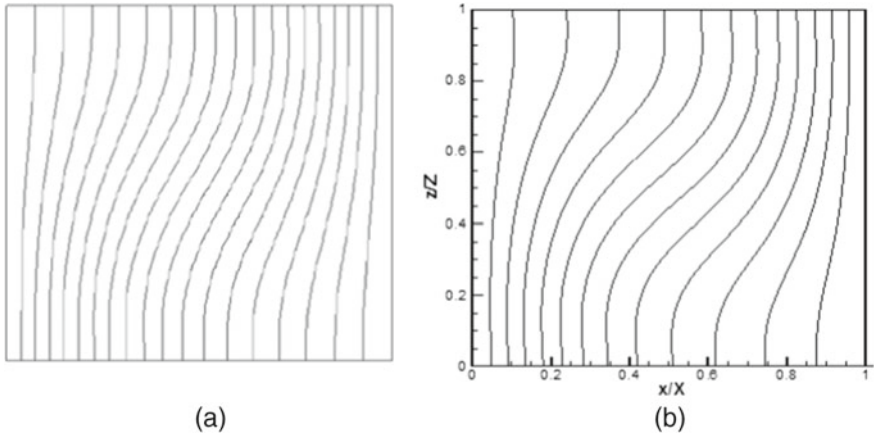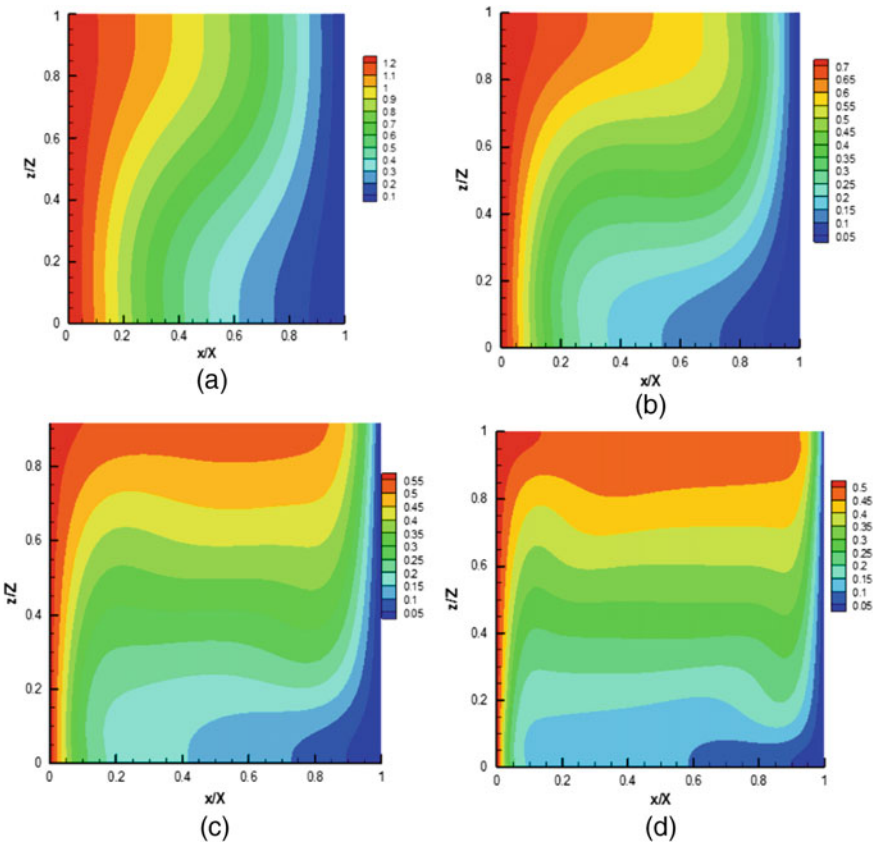
Fig. 10 Isotherms for Ra $= 10^3$ **a** [20] **b** present work

Fig. 11 The predicted temperature contours on the plane of symmetry at different values of Ra: **a** 10^3, **b** 10^4, **c** 10^5, **d** 10^6
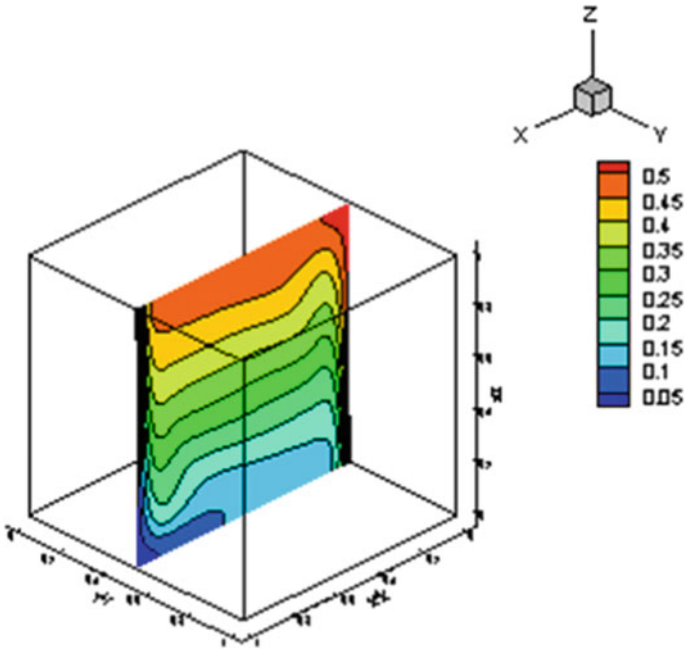
Fig. 12 The contours of temperature in the *x–z* plane of *y/Y* = 0.5 in the cubic cavity for flows of Ra = 10^6
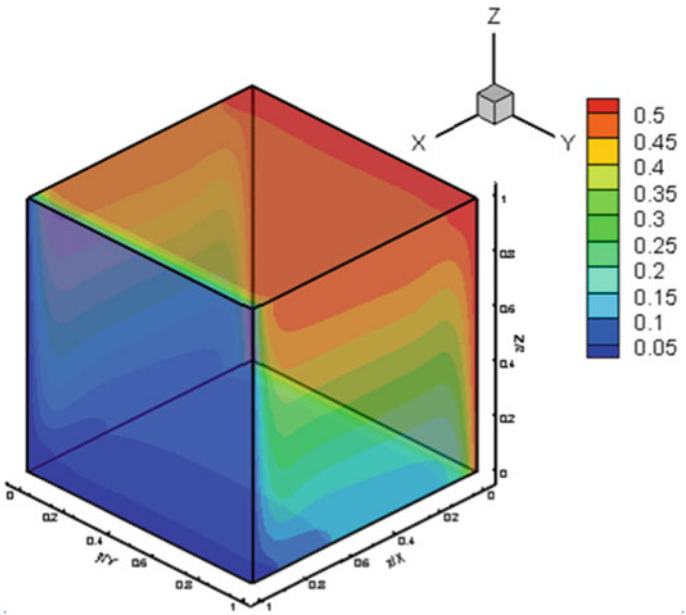

Fig. 13 Iso-surfaces of temperature for Ra = 10^6

allow the expectation that LBM has advantages over conventional energy (convection) equation solvers, especially for problems with complex geometry in multi-dimensional enclosures with axisymmetric or non-axisymmetric diffusive-radiative problems in different multi-mode engineering areas such as multiphase flow and complex fluid phenomena.

References

1. Lee KH, Viskanta R (2001) Two-dimensional combined conduction and radiation heat transfer: comparison of the discrete coordinates method and the diffusion approximation methods. Numer Heat Transf A 39:205–225
2. Razzaque MM, Howell JR, Klein DE (1984) Coupled radiative and conductive heat transfer in a two dimensional enclosure with gray participating media using finite elements. J Heat Transf 106(3):613–619
3. Ho CH, Owisik MN (1988) Combined conduction and radiation in a two-dimensional rectangular enclosure. Numer Heat Transf 13:229–239
4. Rousse DR, Gautier G, Sacadura JF (2000) Numerical prediction of two-dimensional conduction, convection and radiation heat transfer. II-validation Int J ThermSci 39:332–353
5. Wellele O, Orlande HRB, Ruperti N Jr, Colaco MJ, Delmas A (2006) Coupled conduction-radiation in semi-transparent materials at high temperatures. J PhysChem Solids 67:2230–2240
6. Chaabane R, Askri F, Narallah SB (2011) Parametric study of simultaneous transient conduction and radiation in a two-dimensional participating medium. Commun Nonlinear Sci Num Simul 16:4006–4020
7. Chaabane R, Askri F, Narallah SB (2011) A new hybrid algorithm for solving transient combined conduction radiation heat transfer problems. J Thermal Sci 15:649–662
8. Chaabane R, Askri F, Narallah SB (2011) Analysis of two-dimensional transient conduction-radiation problems in an anisotropically scattering participating enclosure using the lattice Boltzmann method and the control volume finite element method. J Comput Phys Commun 182:1402–1413
9. Chaabane R, Askri F, Narallah SB (2011) Application of the lattice Boltzmann method to transient conduction and radiation heat transfer in cylindrical media. J Quant Spectrosc Radiat Transf 112:2013–2027
10. Sakami M, Charette M, Le Dez V (1998) Radiative heat transfer in three dimensional enclosures of complex geometries by using the discrete ordinates method. J Quant Spectrosc Radiat Transf 59:117–136
11. Kang SH, Song T-H (2008) Finite element formulation of the first- and second-order discrete ordinates equations for radiative heat transfer calculation in three-dimensional participating media. J Quant Spectrosc Radiat Transf 109:2094–2107
12. Mishra SC, Lankadasu A, Beronov K (2005) Application of the lattice Boltzmann method for solving the energy equation of a 2-D transient conduction-radiation problem. Int J Heat Mass Transf 48:3648–3659
13. Mishra SC, Roy Hillol K (2007) Solving transient conduction and radiation heat transfer problems using the lattice Boltzmann method and the finite volume method. J Comput Phys 223: 89–107
14. Mishra SC, Mondal B, Kush T, Siva Rama Krishna B (2009) Solving transient heat conduction problems on uniform and non-uniform lattices using the lattice Boltzmann method. Int Commun Heat Mass Transf 36:322–328
15. Mishra SC, Lankadasu A (2005) Analysis of transient conduction and radiation heat transfer using the lattice Boltzmann method and the discrete transfer method. Numer Heat Transf A 47:935–954

16. Mondal B, Mishra SC (2009) Simulation of natural-convection in the presence of volumetric radiation using the lattice Boltzmann method. Numer Heat Transf As 55:18–41
17. Mondal B, Li X (2010) Effect of volumetric radiation on natural convection in a square cavity using lattice Boltzmann method with non-uniform lattices. Int J Heat Mass Transf 5:4935–4948
18. Benzi R, Succi S, Vergassola M (1992) The lattice Boltzmann equation: theory and applications. Phys Rev 222:145–197
19. Mondal B, Siva Rama Krishna B, Mishra SC, Kush T (2009) Solving transient heat conduction problems on uniform and non-uniform lattices using the lattice Boltzmann method. Int Commun Heat Mass Transf 36:322–328
20. NorAzwadi CS, Tanahashi T (2007) Three-dimensional thermal lattice Boltzmann simulation of natural convection in a cubic cavity. Int J Mod Phys B 21:87–96